

RIPPLE PATTERN ANALYSIS IN HERSCHEL CRATER. David A. Vaz^{1,2}, Pedro T.K. Sarmiento^{1,3}, S. Silvestro^{4,5}, M. Cardinale⁶, ¹CITEUC - Centre for Earth and Space Research of the University of Coimbra, Observatório Geofísico e Astronómico da UC, Almas de Freire, 3040-004 Coimbra, Portugal (davidvaz@uc.pt), ²CERENA, Instituto Superior Técnico, Lisboa, Portugal, ³ESAC - European Space and Astronomy Center, Madrid, Spain, ⁴INAF Osservatorio Astronomico di Capodimonte, Napoli, Italy, ⁵Carl Sagan Center, SETI Institute, CA USA, ⁶DiSPUTER, Università Degli Studi G.D'Annunzio, Chieti, Italy.

Introduction: Ripples on Martian dark dune fields are actively migrating and being shaped by near-surface winds [1, 2]. Therefore, they are the bedforms that evolve faster, probably recording even daily wind variations. Complex dune topography should also play an important role, deflecting winds [3, 4] and generating “shadow” zones on the leeward side of the dunes.

HiRISE imagery shows a large diversity of ripple patterns. Some ripple sets form regular arrays of straight elongated bedforms, while others can present sinuous traces, resembling linguoid or lunate ripples described in subaqueous environments [5]. Our aim is to understand the meaning of these pattern variations. To achieve this, we have created a dataset that allows the correlation of ripple pattern characteristics, morphometric parameters, migration rates, and a simplified wind effect model [6]. Here we present a preliminary analysis of this integrated dataset.

Data and methodologies: The base data for this work are HiRISE DTMs and orthorectified images. COSI-Corr was used to estimate ripple migrations, and the DTM was used to model the wind effect on the topography [6]. Using the OBRA (Object-Based Ripple Analysis) ripple mapping technique [7] we mapped the ripples on a 15 km² area located in Herschel Crater (Fig. 1). The studied dune field consists of asymmetric barchans and barchanoids, with slipfaces elongated obliquely [8].

A regular grid with 10 m spacing was created to integrate the ripple patterns characteristics (length, wavelength, circular mean, modes, circular dispersion, etc.), morphometric parameters (slopes, aspect angles, etc.), migration (magnitude and trend) and a wind effect index. The obtained dataset provides the spatial integration of all these data sources, being ideal to test possible pattern correlations over large areas (Fig. 1).

Results: The compiled dataset combine a large variety of parameters. A complete analysis must then make use of multivariate statistical methods, such as PCA, clustering or multivariate correlations. Here we will simply discuss a first exploratory data analysis, focusing the discussion on one pattern characteristic: the average length of the ripples.

Figures 1b and c show the spatial distribution of the average ripple length. Clusters of ripples presenting higher lengths are visible, suggesting that the spatial

distribution of this variable is clearly not random. A North-South variation is also apparent, with a larger concentration of these clusters in the Northern region.

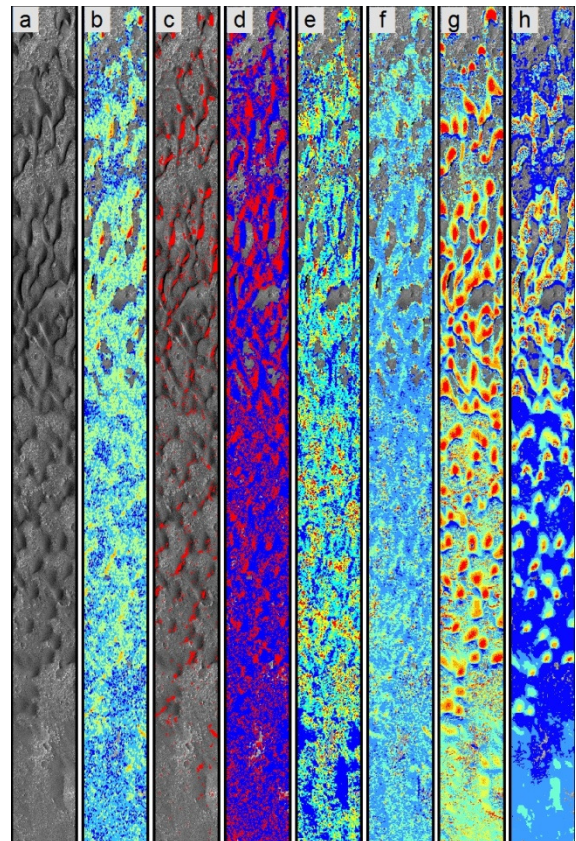


Figure 1 – Study area with some examples of the parameters that were computed. a) HiRISE image; b) average ripple length, note the clusters of longer ripples; c) location of the ripple clusters with average lengths higher than 9 m; d) azimuth of the primary mode, see Fig. 2 for a detailed view of this parameter (N0°-N90° in blue, N90°-N180° in red); e) directional strength ratio; f) ripple average wavelength; g) wind effect on the topography assuming winds blowing from N0°±30°, note the stronger effect of the wind in the windward section of the dunes, and the sheltered areas located in the leeward side of the slipfaces; h) magnitude of the COSI-Corr migration vectors, these seem to be positively correlated with the modeled wind effect index.

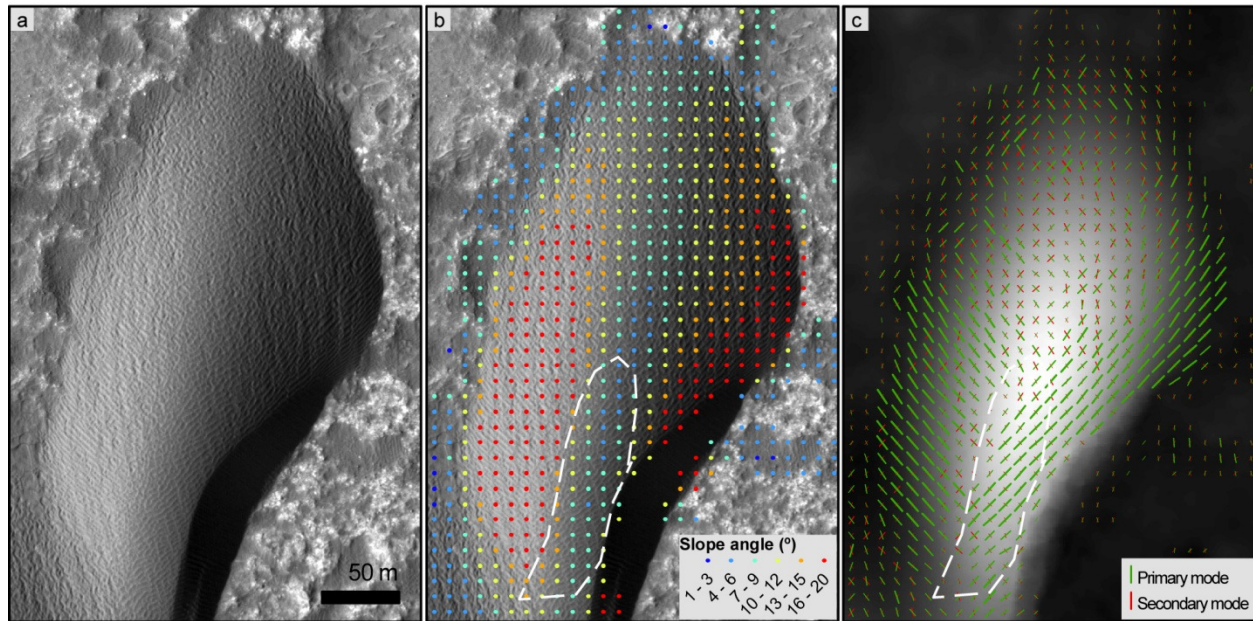


Figure 2 – Detailed view of the ripple pattern over an asymmetric barchan. a) HiRISE image; b) surface slope angle; c) ripple pattern modal trends (primary and secondary modes in green and red respectively), the length of the traces correspond to the kernel modal strength. In this case, nearly orthogonal ripple sets coexist in the stoss slope. Longer ripples seem to be well correlated with higher slopes, but on the dashed area, longer ripples also occur in a relatively flat crest area.

The sub-population of ripples with average lengths higher than 9 m (Fig. 1c) corresponds to sets of long and straight ripples with an average wavelength of 2.6 ± 0.4 m. As shown in Fig. 1c, this sub-population represents a small percentage of the total population (circa 5%). More commonly, the ripples are short and appear in almost orthogonal sets that coexist in the same area.

In most of the cases, the clusters of long ripples appear associated with: 1) dune flanks, in areas presenting higher slopes and with $\sim N45^\circ$ and $\sim N145^\circ$ trends (Fig. 2); 2) leeside of dome dunes, particularly in the southern region; 3) at the base of slipfaces, where they can sometimes present a North-South trend.

Discussion and conclusion: The example given in this report highlights the use of automated ripple pattern characterization tools for the systematic study of pattern spatial variations. We have limited our analysis only to the average length of the ripples, a pattern characteristic which is considered to be influenced by bed shear stress (straight ripples were associated with lower flow velocities for subaqueous ripples [5]) or across-crest transport flows [9]. The location and morphometric context of the clusters of long and straight ripples that we have identified at Herschel, seems to be consistent with these possible explanations. The association with higher slopes is particularly evident, indi-

cating that gravitational slope transport may be occurring, generating the elongation of the ripples. However, the same physical mechanism cannot be invoked for the other contexts, where upstream topographic obstacles seem to be relevant [10].

References: [1] Silvestro S., et al. (2013). *Geology*, Vol. 41 (4),483-486. [2] Silvestro S., et al. (2011). *Geophys. Res. Lett.*, Vol. 38 (20),L20201. [3] Howard A. D. (1977). *Geol. Soc. Am. Bull.*, Vol. 88,853-856. [4] Zimelman J. R. and M. B. Johnson (2015). *LPSC 2015*, Abstract 1478. [5] Allen J. R. L., *Current ripples; their relation to patterns of water and sediment motion*. Amsterdam, North-Holland Pub. Co., 1968. [6] Winstral A., et al. (2002). *J Hydrometeorol*, Vol. 3 (5),524-538. [7] Vaz D. A. and S. Silvestro (2014). *Icarus*, Vol. 230,151-161. [8] Cardinale M., et al. (2012). *Earth Surface Processes and Landforms*, Vol. 37 (13),1437-1443. [9] Rubin D. M. (2012). *Earth-Sci Rev*, Vol. 113 (3-4),176-185. [10] Silvestro S., et al. (2015). This volume.

Acknowledgements: This work was supported by FCT (Fundação para a Ciência e a Tecnologia) with the grant FRH/BPD/72371/2010 and the contracts PESt-OE/CTE/UI0611/2012-CGUC and PTDC/CTE-SPA/117786/2010.